International Journal of Solids and Structures 50 (2013) 4080–4088

Contents lists available at ScienceDirect

International Journal of Solids and Structures

journal homepage: www.elsevier.com/locate/ijsolstr

Application of the reciprocity theorem to scattering of surface waves by a cavity

Haidang Phan [a], Younho Cho [a,*], Jan D. Achenbach [b]

[a] School of Mechanical Engineering, Pusan National University, Pusan, South Korea
[b] Center for Quality Engineering & Failure Prevention, Northwestern University, Evanston, IL, USA

ARTICLE INFO

Article history:
Received 29 September 2012
Received in revised form 13 August 2013
Available online 27 August 2013

Keywords:
Surface wave
Cavity
Half-space
Reciprocity theorem
BEM

ABSTRACT

Scattering of surface waves by a cylindrical cavity at the surface of a homogenous, isotropic, linearly elastic half-space is analyzed in this paper. In the usual manner, the scattered field is shown to be equivalent to the radiation from a distribution of tractions, obtained from the incident wave on the surface of the cavity. For the approximation used in this paper, these tractions are shifted to tractions applied to the projection of the cavity on the surface of the half-space. The radiation of surface waves from a normal and a tangential line load, recently determined by the use of the reciprocity theorem, is employed to obtain the field scattered by the cavity from the superposition of displacements due to the distributed surface tractions. The vertical displacement at some distance from the cavity is compared with the solution of the scattering problem obtained by the boundary element method (BEM) for various depths and widths of the cavity. Comparisons between the analytical and BEM results are graphically displayed. The limitations of the approximate approach are discussed based on the comparisons with the BEM results.

1. Introduction

Corrosion is a very undesirable damage mechanism in a wide variety of practical structures. It has the potential to grow in volume over time and tends to generate corrosion pits, i.e., small cavities at the surface of structural elements. It is, therefore, important that corrosion pits are detected for timely repair or replacement of affected structural components. When a surface with corrosion pits is not accessible for visual inspection, guided ultrasonic waves, such as surface waves, can be very useful in the detection and characterization of corrosion pits.

The principal purpose of the present paper is to use the surface waves generated by time-harmonic normal and tangential line loads, applied to the free surface, recently determined by the use of the reciprocity theorem, (Achenbach, 2003), in combination with a shift of tractions on the cavity to the free surface, to analyze the forward and backscattering of a surface wave by a single surface cavity. The surface wave obtained by the reciprocity approach is in simpler form compared with the solution by Lamb's approach even though it can be shown that the expressions can be converted to each other (Phan et al., 2013). As a result, simpler expressions for the scattered field are obtained. In principle, this approach is applicable for a cavity of arbitrary shape. To determine the advantages and the limits of applicability of the proposed method, however, we consider a relatively simple two-dimensional configuration of scattering by a cylindrical cavity at the surface of a homogeneous, isotropic, linearly elastic half-space. It is discussed at what cavity-depth and cavity-width the approximation begins to diverge significantly from an exact numerical solution of the scattering problem obtained by the boundary element method.

The description of the approach proposed in this paper proceeds through eight sections. Section 2 states the problem as the superposition of the incident wave and the scattered field. It is shown that the scattered field is equivalent to the field radiated by surface tractions on the surface of the cavity. These surface tractions are obtained from the incident wave. Next, the principal approximation, the shifting of these surface tractions to the surface of an intact half-space, is applied. Section 3 presents the relevant expressions for Rayleigh waves on an elastic half-space. A method to determine the displacement field of the surface wave radiated by a surface force using the reciprocity theorem; see the book by Achenbach (2003), is discussed in Section 4. The validity of the method using the reciprocity theorem is verified by comparison with the classical solution based on the application of the integral transform technique; see Phan et al. (2013). In Section 5, the application of the method of Sections 2–4 to scattering by a surface cavity of arbitrary shape is discussed. Section 6 presents details for scattering by a cylindrical cavity. Section 7 briefly discusses the use of the boundary element method. Finally, in Section 8, detailed results, comparisons and conclusions are presented for scattering by a cylindrical cavity. The comparisons

* Corresponding author.
E-mail address: mechcyh@pusan.ac.kr (Y. Cho).

0020-7683/$ - see front matter © 2013 Elsevier Ltd. All rights reserved.
http://dx.doi.org/10.1016/j.ijsolstr.2013.08.020

with the BEM results for different cavities display limitations of the approximate approach.

With respect to earlier work on scattering of surface waves by surface defects, much of the work in the literature has been concerned with scattering by surface breaking cracks. Typical example of analytical work is the paper by Auld (1979). Numerical work has been carried out by the finite element method; see Hassan and Veronesi (2003), and the boundary element method; see Arias and Achenbach (2004). In a related category are papers on scattering by strips and grooves, by Gregory and Austin (1990), Kosachev et al. (1990), Simons (1978), Tuan and Li (1974). The radiation of surface waves from a pressurized surface cavity by Phan et al. (2013) has features in common with the scattering of an incident surface wave by a cavity. Good agreement between numerical and experimental results of Rayleigh waves scattered by surface defects can be found in Viktorov (1970).

The approximate boundary conditions of shifting the loading of the cavity on the flat surface was earlier explored by Gilbert and Knopoff (1960), see also Ogilvy's review article (Ogilvy, 1987). An approach based on matched asymptotic expansions was presented by Abrahams and Wickham (1992).

It is of interest to note differences in the approach by Gilbert and Knopoff (1960) and the present paper. In their 1960 paper Gilbert and Knopoff primarily considered a hill, but their approach also applies to a cavity. For a cavity both papers determine the distribution of tractions on the cavity surface, due to the incident wave. The negative of these tractions generate the scattered field. In the present paper, no initial assumptions are made on the depth and width of the cavity, and the calculated distributions of tractions are directly shifted to the projection of the cavity on the free surface. Gilbert and Knopoff, on the other hand, first expand the traction distributions in two-term Taylor expansions with respect to the free surface, for small cavity depth and slope, before shifting to the free surface. This requires an immediate assumption that the depth and the slope of the cavity are small as compared to the wavelength. The scattered field is then calculated by using Lamb's complicated solutions for waves generated by line loads on a half-space. The present paper is interested in scattered surface waves, and it uses a recently developed simple closed-form expression for the surface waves generated by time-harmonic line loads applied normal and tangential to the free surface. The resulting superposition integrals for the distributions of the shifted tractions are easy to compute for a number of depths and widths of the cavity. By comparison with results obtained by the boundary element method, limits of validity for depth and width have $z \geq 0$ been obtained for a cylindrical cavity.

The related problem of scattering of Lamb waves by a surface defect in a layer has received considerable attention; see e.g. the papers by Cho and Rose (2000), and Moreau and Castaings (2008), which both list several other contributions. We also mention a recent paper by Hao et al. (2011), which is concerned with a problem closely related to the problem discussed in the present paper, but where the distributions of tractions on a cavity in a layer are represented by single resultant forces applied to the surface of the intact layer.

2. Statement of the problem

A homogeneous, isotropic, linearly elastic solid which occupies the half-space, relative to a Cartesian coordinate system, (x, y, z), contains a cylindrical surface cavity in the x, z-plane. A plane surface wave propagating in the x-direction is incident on the cavity, see Fig. 1a. The interaction of the surface wave with the cavity generates forward-scattered and back-scattered surface waves which are investigated in this paper. The total field may be written as

$$\mathbf{u}_{tot} = \mathbf{u}_{in} + \mathbf{u}_{sc} \tag{1}$$

where the three fields are the total, the incident and the scattered fields.

By virtue of linear superposition shown in Fig. 1, the scattered field is equivalent to the field generated by the application of a distribution of horizontal and vertical tractions on the surface of the cavity. These tractions are equal in magnitude but opposite in sign to the corresponding tractions due to the incident wave on a virtual cavity in the half-space without cavity. Thus, the horizontal and vertical tractions can be calculated from the stress components of the incident Rayleigh wave and the outward normal vectors of the cavity surface by using Cauchy's formula. The tractions, in turn, generate a radiated field which is equivalent to the scattered wave field. It is noted that the tractions on the surface of the cavity generate body waves as well as surface waves. The surface waves, which do not suffer geometrical attenuation, dominate at sufficiently large values of $|x|$.

In a simple approximation the tractions acting on the cavity surface can be replaced by a resultant vertical load and a resultant horizontal load applied at the origin of the coordinate system, as long as the cavity depth and width are both much smaller than the incident wavelength. This approximation is simple in calcula-

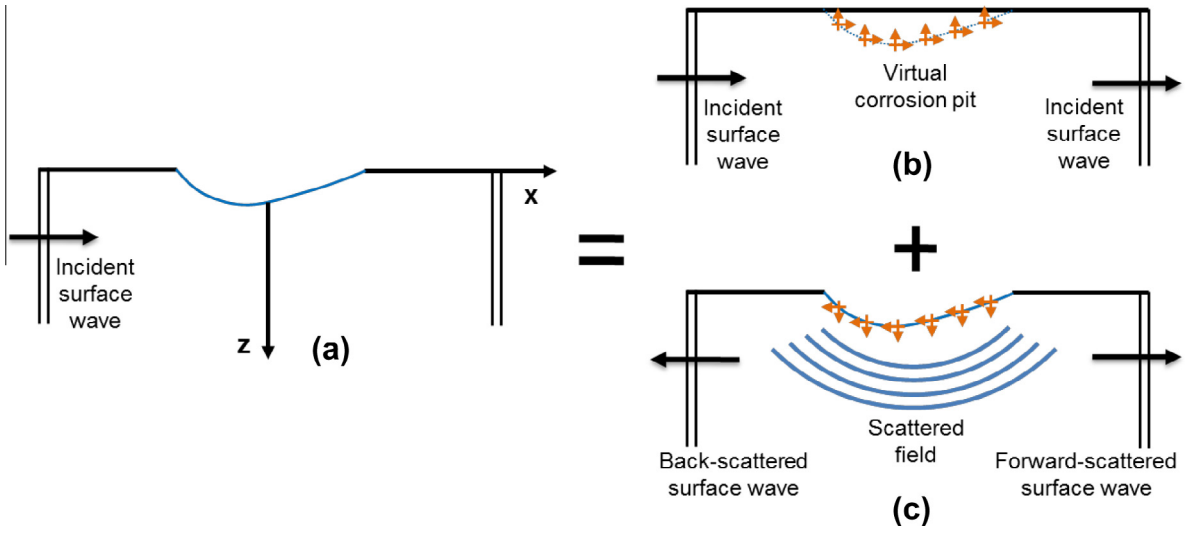

Fig. 1. Linear superposition principle.

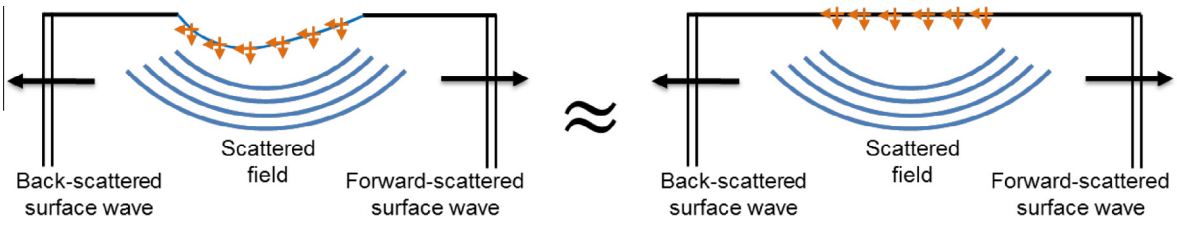

Fig. 2. Analytical solution approximated by the reciprocity.

tion but less accurate when the cavity depth and width are comparable to the incident wavelength. As an improvement, the scattered field generated by the application of the distribution of tractions shifted to the surface of the half-space is determined in this paper, see Fig. 2.

The traction components are first calculated for every point of the cavity surface. The reciprocity theorem is then applied to the equivalent loads that are applied on the surface of the half-space, to obtain the displacement amplitudes of the scattered field. The total displacement amplitude is a superposition of the amplitudes generated by the horizontal and vertical loads at every point on the surface.

3. Rayleigh waves in an elastic half-space

Surface waves, traveling along the free surface of an elastic half-space, whose displacements decay exponentially with distance from the free surface, were first investigated by Rayleigh (1885). The classical surface waves considered here are two-dimensional and nondispersive. There is much literature on this subject including, for example, Achenbach (1973), Ewing et al. (1957). In addition that the amplitude decreases with depth, a surface wave is defined by an angular frequency ω and a wavenumber k, where $k = \omega/c$, c being the surface wave velocity, as well as material properties λ, μ, ρ. The displacements of surface waves may be written as

$$u_x = \pm iAU^R(z)e^{\pm ikx}, \quad u_z = AW^R(z)e^{\pm ikx} \tag{2a, b}$$

where the term $\exp(i\omega t)$ has been omitted, and the plus and minus signs apply to Rayleigh waves traveling in the negative and positive x-direction, respectively. In Eqs. (2a, b)

$$U^R(z) = d_1 e^{-kpz} + d_2 e^{-kqz} \tag{3}$$

$$W^R(z) = d_3 e^{-kpz} - e^{-kqz} \tag{4}$$

where

$$d_1 = \frac{-(1+q^2)}{2p}, \quad d_2 = q, \quad d_3 = \frac{1+q^2}{2} \tag{5}$$

Here

$$p = \sqrt{1 - c^2/c_L^2}, \quad q = \sqrt{1 - c^2/c_T^2} \tag{6}$$

while

$$c_L = \sqrt{(\lambda + 2\mu)/\rho}, \quad c_T = \sqrt{\mu/\rho} \tag{7}$$

are the longitudinal and transverse wave velocities, respectively. The corresponding stresses can be written as

$$\tau_{xx} = AT_{xx}^R(z)e^{\pm ikx} \tag{8}$$

$$\tau_{xz} = \pm iAT_{xz}^R(z)e^{\pm ikx} = \tau_{zx} \tag{9}$$

$$\tau_{zz} = AT_{zz}^R(z)e^{\pm ikx} \tag{10}$$

where

$$T_{xx}^R(z) = k\mu(d_4 e^{-kpz} + d_5 e^{-kqz}) \tag{11}$$

$$T_{xz}^R(z) = k\mu(d_6 e^{-kpz} + d_7 e^{-kqz}) = T_{zx}^R(z) \tag{12}$$

$$T_{zz}^R(z) = k\mu(d_8 e^{-kpz} + d_9 e^{-kqz}) \tag{13}$$

with

$$d_4 = \frac{(1+q^2)(1+2p^2-q^2)}{2p}, \quad d_5 = -2q, \quad d_6 = 1+q^2 \tag{14}$$

$$d_7 = -(1+q^2), \quad d_8 = -2q, \quad d_9 = 2q \tag{15}$$

In Eqs. (8)–(13), $k = \omega/c$ is a wavenumber-like quantity. It should also be noted that p, q and $d_1 - d_9$ are dimensionless quantities.

The boundary conditions at $z = 0$, which are

$$\tau_{zz}(x,0) = 0, \quad \tau_{zx}(x,0) = 0 \tag{16a, b}$$

yield the following well-known equation for the phase velocity of the surface waves

$$\left(2 - \frac{c^2}{c_T^2}\right)^2 - 4\sqrt{1 - \frac{c^2}{c_L^2}}\sqrt{1 - \frac{c^2}{c_T^2}} = 0 \tag{17}$$

4. Radiation from surface forces

Of the classical problems in elastodynamics, the surface wave motion radiated from a concentrated load at the surface of a half-space is arguably the one of most significance. The problem was first solved by Lamb (1904) who fully investigated the surface motions generated by a line load and a point load applied normally to the surface. The methods and solutions of Lamb's paper were cast in a somewhat more elegant form and more detailed computations were carried out, particularly for loads of arbitrary time dependence; see Achenbach (1973), Ewing et al. (1957). These solutions were found based on the use of the Fourier transform techniques. For the two-dimensional case of an applied line load, which is of interest for this paper, the solution was given in terms of integrals along branch cuts for the body waves, and the residues of poles for the surface waves.

The Fourier transform approach, however, becomes more difficult for anisotropic solids, and is impossible for inhomogeneous solids, for example, solids whose elastic moduli depend on the depth coordinate, as is the case for geophysical applications and functionally graded materials. To avoid these difficulties, another method has been proposed in recent years, based on the elastodynamic reciprocity theorem, strictly to determine the surface waves, see Achenbach (2000, 2003), Phan et al. (2013). It has been shown that the method based on the reciprocity theorem is exceedingly simple, and gives the same result as obtained by the Fourier transform techniques.

In general, the elastodynamic reciprocity theorem provides a relation between displacements, traction components and body forces for two different states of the same body. For the two-

dimensional case of time-harmonic quantities, the relation is of the form

$$\int_V \left(f_j^A u_j^B - f_j^B u_j^A\right) dV = \int_S \left(\tau_{ij}^B u_j^A - \tau_{ij}^A u_j^B\right) n_i dS \tag{18}$$

where S defines a contour around an area defined by V, and f_j, u_j and τ_{ij} denote the components of forces, displacements and stresses, respectively. Here the superscripts A and B denote two elastodynamic states. For the radiated field generated by a single surface force, two elastodynamic states, one of which is the surface wave of the radiated wave field and the other is a free virtual surface wave, are connected by Eq. (18). This integral relation then makes it possible to obtain the radiated amplitudes with a much simpler calculation as compared with the Fourier transform approach.

In this section, we summarize the results from Phan et al. (2013) to obtain the scattered amplitudes of the surface waves radiated by a time-harmonic line load. We first consider a vertical force applied on the surface of the half-space at x_0

$$f_z^A = P\delta(z)\delta(x - x_0) \tag{19}$$

where the term $\exp(i\omega t)$ has been omitted. Following from (Phan et al., 2013), the scattered amplitude in the negative x-direction may be written as

$$A_P^- = \frac{iPW^R(0)}{2\mu E} \tag{20}$$

and

$$u_z^{A-}(x,z) = \frac{iPW^R(0)}{2\mu E} e^{-ikx_0} W^R(z) e^{ikx} \tag{21}$$

The scattered amplitude in the positive x-direction is

$$A_P^+ = \frac{iPW^R(0)}{2\mu E} \tag{22}$$

and

$$u_z^{A+}(x,z) = \frac{iPW^R(0)}{2\mu E} e^{ikx_0} W^R(z) e^{-ikx} \tag{23}$$

Similarly, for a horizontal force applied on the surface at x_0

$$f_x^A = Q\delta(z)\delta(x - x_0) \tag{24}$$

we find the scattered amplitude in the negative x-direction

$$A_Q^- = \frac{QU^R(0)}{2\mu E} \tag{25}$$

and

$$u_z^{A-}(x,z) = \frac{QU^R(0)}{2\mu E} e^{-ikx_0} W^R(z) e^{ikx} \tag{26}$$

Also, we obtain the scattered amplitude in the positive x -direction

$$A_Q^+ = -\frac{QU^R(0)}{2\mu E} \tag{27}$$

and

$$u_z^{A+}(x,z) = -\frac{QU^R(0)}{2\mu E} e^{ikx_0} W^R(z) e^{-ikx} \tag{28}$$

In Eqs. (20)–(23) and Eqs. (25)–(28), E can be evaluated as

$$E = \frac{d_1 d_4 - d_3 d_6}{2p} + \frac{d_2 d_4 + d_1 d_5 - d_3 d_7 + d_6}{p+q} + \frac{d_2 d_5 + d_7}{2q} \tag{29}$$

A line load on an elastic half-space generates cylindrical longitudinal and transverse waves, as well as surface waves. It is remarkable that an application of the reciprocity theorem just using the surface waves generated by the line load for state A together with a virtual surface wave for state B yields the correct amplitudes for the surface waves of state A.

It was proved in Phan et al. (2013) that the methods of the reciprocity theorem and the integral transform technique to obtain the solution of the surface wave motion yield the same result.

5. Application to scattering by a cavity of arbitrary shape

In this section the approximate approach to the analysis of surface waves scattered by a cavity at the surface of an elastic half-space is applied to a cavity that has a smooth boundary, but is otherwise of arbitrary shape. The shape of the cavity is defined by

$$z = h(x) \tag{30}$$

The displacements of the incident surface wave are defined by Eq. (2a, b), and the corresponding stresses are given by Eqs. (8)–(10), taking into account the suitable signs. The boundary of the virtual cavity, together with an element dA at the boundary, is shown in Fig. 3.

The horizontal force calculated on the virtual cavity boundary at (x_0, z_0) is

$$f_x(x_0,z_0) = \tau_{xx}(x_0,z_0)h'(x_0)dx_0 - \tau_{xz}(x_0,z_0)dx_0 \tag{31}$$

and the vertical force is

$$f_z(x_0,z_0) = \tau_{xz}(x_0,z_0)h'(x_0)dx_0 - \tau_{zz}(x_0,z_0)dx_0 \tag{32}$$

Substitution of $\tau_{xx}(x_0,z_0)$, $\tau_{xz}(x_0,z_0)$ and $\tau_{zz}(x_0,z_0)$ from Eqs. (8)–(10), taking into account the suitable signs, into Eqs. (31) and (32) yields

$$f_x(x_0,z_0) = -A_{in}\left[T_{xx}^R(z_0)h'(x_0) + iT_{xz}^R(z_0)\right] e^{-ikx_0} dx_0 \tag{33}$$

and

$$f_z(x_0,z_0) = -A_{in}\left[iT_{xz}^R(z_0)h'(x_0) + T_{zz}^R(z_0)\right] e^{-ikx_0} dx_0 \tag{34}$$

where A_{in} is the amplitude of the incident wave, and

$$z_0 = h(x_0) \tag{35}$$

The radiation from the opposites in sign of the distributions with respect to x_0 of these surface forces approximates the scattering of an incident surface wave by the cavity. The forward radiation of the displacement in the z-direction generated by $-f_z(x_0,z_0)$ follows as the sum of Eqs. (23) and (28) with Pe^{ikx_0} replaced by $-f_z(x_0,z_0)$ and Qe^{ikx_0} by $-f_x(x_0,z_0)$. Similarly, the backward radiation follows as the sum of Eqs. (21) and (26). The results are for $x > 0$:

$$u_z^{A+}(x,z) = \frac{iA^+(x_0,z_0)}{2I} F^+(x_0,z_0)dx_0 W^R(z)e^{-ikx} \tag{36}$$

are for $x < 0$:

$$u_z^{A-}(x,z) = \frac{iA^-(x_0,z_0)}{2I} F^-(x_0,z_0)e^{-2ikx_0}dx_0 W^R(z)e^{ikx} \tag{37}$$

where

$$F^+(x_0,z_0) = i\left[T_{xx}(z_0)h'(x_0) + iT_{xz}(z_0)\right]U^R(0) - \left[iT_{xz}(z_0)h'(x_0) + T_{zz}(z_0)\right]W^R(0) \tag{38}$$

$$F^-(x_0,z_0) = -i\left[T_{xx}(z_0)h'(x_0) + iT_{xz}(z_0)\right]U^R(0) - \left[iT_{xz}(z_0)h'(x_0) + T_{zz}(z_0)\right]W^R(0) \tag{39}$$

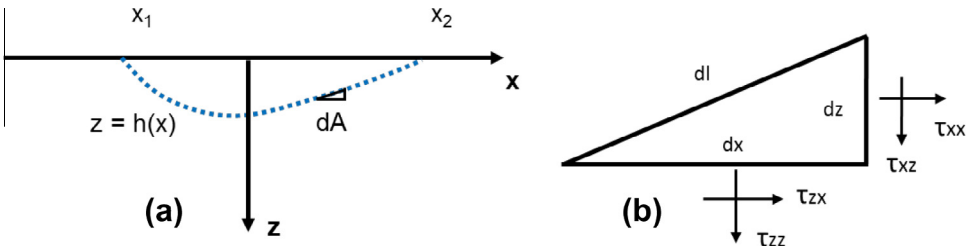

Fig. 3. Virtual cavity (a) and element for stress analysis (b).

Equations (36) and (37) just represent the radiation from individual surface forces located at $x = x_0$. To obtain the radiation of the distributions of surface forces, Eqs. (36) and (37) must be integrated over x_0 from $x_0 = x_1$ to $x_0 = x_2$, see Fig. 3. On the surface ($z = 0$), we have

$$u_z^{A+} = A_{sc}^{+} W^R(0) e^{-ikx} \tag{40}$$

$$u_z^{A-} = A_{sc}^{-} W^R(0) e^{ikx} \tag{41}$$

where

$$\frac{A_{sc}^{-}}{A_{in}} = \frac{i}{2I} \int_{x_1}^{x_2} F^{-}(x_0, z_0) e^{-2ikx_0} dx_0 \tag{42}$$

$$\frac{A_{sc}^{+}}{A_{in}} = \frac{i}{2I} \int_{x_1}^{x_2} F^{+}(x_0, z_0) dx_0 \tag{43}$$

In these expressions, z_0 is defined in terms of x_0 by Eq. (35).

6. Example: scattering by a cylindrical cavity

As an example we consider the scattering of the surface wave by a cylindrical cavity at the surface of a half-space. The two-dimensional geometry of the cavity, which has a depth D and a width $2R_0$ is shown in Fig. 4. The Cartesian coordinate system is chosen such that the plane $z = 0$ coincides with the surface of the half-space.

Two relations between R, Z and R_0 follow from the geometry

$$R^2 = Z^2 + R_0^2 \quad \text{and} \quad Z = R - D \tag{44}$$

By combining these two relations we find

$$R = \frac{R_0^2 + D^2}{2D} \tag{45}$$

$$Z = \frac{R_0^2 - D^2}{2D} \tag{46}$$

and

$$z_0 = h(x_0) = \left(R^2 - x_0^2\right)^{1/2} - Z \tag{47}$$

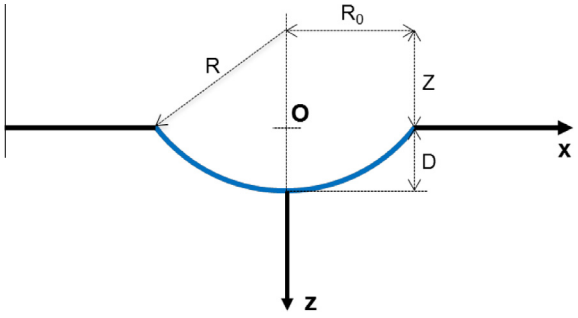

Fig. 4. Cavity geometry.

$$h'(x_0) = -\frac{x_0}{\left(R^2 - x_0^2\right)^{1/2}} \tag{48}$$

It is more useful to introduce dimensionless variables

$$\bar{x}_0 = kx_0, \quad \bar{z}_0 = kz_0, \quad \bar{R} = kR, \quad \bar{R}_0 = kR_0, \quad \bar{D} = kD, \quad \bar{Z} = kZ \tag{49}$$

Equations (45), (46) become

$$\bar{R} = \frac{\bar{R}_0^2 + \bar{D}^2}{2\bar{D}}, \quad \bar{Z} = \frac{\bar{R}_0^2 - \bar{D}^2}{2\bar{D}} \tag{50}$$

and (47), (48) become

$$\bar{z}_0 = \left(\bar{R}^2 - \bar{x}_0^2\right)^{1/2} - \bar{Z} \tag{51}$$

$$h'(\bar{x}_0) = -\frac{\bar{x}_0}{\left(\bar{R}_0^2 - \bar{x}_0^2\right)^{1/2}} \tag{52}$$

Eqs. (42) and (43) can now be written

$$\frac{A_{sc}^{-}}{A_{in}} = \frac{i}{2E} \int_{-\bar{R}_0}^{\bar{R}_0} \bar{F}^{-}(\bar{x}_0, \bar{z}_0) e^{-2i\bar{x}_0} d\bar{x}_0 \tag{53}$$

$$\frac{A_{sc}^{+}}{A_{in}} = \frac{i}{2E} \int_{-\bar{R}_0}^{\bar{R}_0} \bar{F}^{+}(\bar{x}_0, \bar{z}_0) d\bar{x}_0 \tag{54}$$

where

$$\begin{aligned} \bar{F}^{+}(x_0, z_0) = {} & \left[\left(d_6 e^{-p\bar{z}_0} + d_7 e^{-q\bar{z}_0}\right)(d_1 + d_2)\right. \\ & \left. -\left(d_8 e^{-p\bar{z}_0} + d_9 e^{-q\bar{z}_0}\right)(d_3 - 1)\right] \\ & + i \frac{\bar{x}_0}{\left(\bar{R}_0^2 - \bar{x}_0^2\right)^{1/2}} \left[-\left(d_4 e^{-p\bar{z}_0} + d_5 e^{-q\bar{z}_0}\right)(d_1 + d_2)\right. \\ & \left. +\left(d_6 e^{-p\bar{z}_0} + d_7 e^{-q\bar{z}_0}\right)(d_3 - 1)\right] \end{aligned} \tag{55}$$

and

$$\begin{aligned} \bar{F}^{-}(x_0, z_0) = {} & \left[-\left(d_6 e^{-p\bar{z}_0} + d_7 e^{-q\bar{z}_0}\right)(d_1 + d_2)\right. \\ & \left. -\left(d_8 e^{-p\bar{z}_0} + d_9 e^{-q\bar{z}_0}\right)(d_3 - 1)\right] \\ & + i \frac{\bar{x}_0}{\left(\bar{R}_0^2 - \bar{x}_0^2\right)^{1/2}} \left[\left(d_4 e^{-p\bar{z}_0} + d_5 e^{-q\bar{z}_0}\right)(d_1 + d_2)\right. \\ & \left. +\left(d_6 e^{-p\bar{z}_0} + d_7 e^{-q\bar{z}_0}\right)(d_3 - 1)\right] \end{aligned} \tag{56}$$

Note that all quantities of Eqs. (53)–(56) are dimensionless, and $\bar{z}_0$ is given in Eq. (51) while E is given in Eq. (29).

7. Boundary element method

The boundary element method (BEM) is used in this paper to obtain numerical results for comparison with the analytical solutions. BEM, which only requires the discretization of the boundary, is ideally suited for the numerical analysis of problems of wave scattering by flaws such as cracks, cavities and inclusions in elastic media that are unbounded outside the bounded domain of the

scatterer. However, when the body is a half-space, with cracks, voids and cavities, not only the domain but also its boundary are unbounded. Therefore, for the BEM formulation of a half-space, the surface of the half-space generally has to be discretized to enforce the appropriate boundary conditions. In this paper the Rayleigh wave correction for the BEM analysis of two-dimensional elastodynamic problems in a half-space presented by Arias and Achenbach (2004) is applied to correct the error introduced by the truncation of the boundary. In this approach, it is assumed that the numerical solution takes the far-field form of a Rayleigh wave of unknown amplitude and phase on the omitted part of the boundary. This assumption is used here to rewrite the integrals that represent the contribution of the omitted part or the boundary as the product of integrals of known quantities on the omitted part of the boundary and the unknown amplitudes and phases of the far-field Rayleigh waves. In order to eliminate these unknowns, the assumed far-field Rayleigh waves are matched to the nodal values at the end nodes of the computational boundary. Consequently, the coefficients of the original BEM displacement system matrix associated with the end nodes are modified.

Depending on the idea of Rayleigh wave correction presented in Arias and Achenbach (2004), a BEM code has been written in FORTRAN to simulate the two-dimensional scattering of surface waves by a surface cavity in a half-space. The boundary conditions applying for the scattered field are the traction values obtained theoretically at the positions of the cavity boundary but of the opposite sign. With this idea, the problem has been solved numerically by the direct frequency domain boundary element method which allows the Rayleigh waves propagating along the free surface of the half-space to escape the computational domain without producing spurious reflections from its limits.

8. Results and conclusions

The absolute values of the amplitude ratios from Eqs. (53) and (54), given by

$$\left|\frac{A_{sc}^{-}}{A_{in}}\right| = \frac{i}{2E}\int_{-\bar{R}_0}^{\bar{R}_0} \bar{F}^{-}(\bar{x}_0,\bar{z}_0)e^{-2i\bar{x}_0}d\bar{x}_0 \tag{57}$$

$$\left|\frac{A_{sc}^{+}}{A_{in}}\right| = \frac{i}{2E}\int_{-\bar{R}_0}^{\bar{R}_0} \bar{F}^{+}(\bar{x}_0,\bar{z}_0)d\bar{x}_0 \tag{58}$$

are plotted for different cylindrical cavities in comparison with numerical results obtained by the boundary element method. The BEM results presented here are close to the exact solutions. The comparisons are plotted vs. the dimensionless quantities $kD = \bar{D}$ and $kR_0 = \bar{R}_0$. We also impose the condition for the cavities that

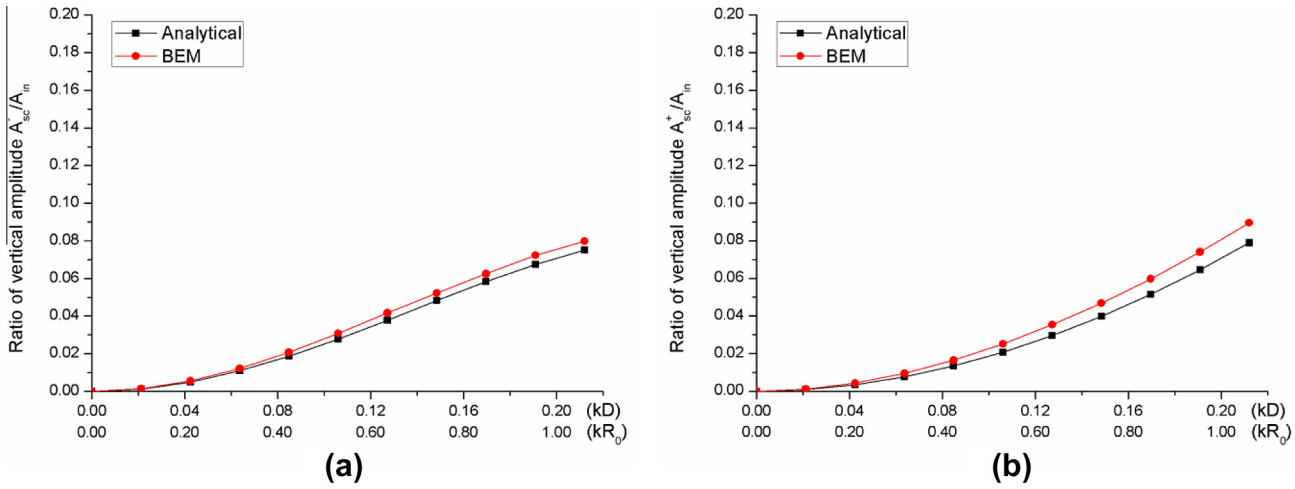

Fig. 5. Scattering by a cylindrical cavity; $R_0 = 0.50$ mm, $D = 0.10$ mm, 0.1 MHz $\leq f \leq$ 1.0*MHz*; (a) Backscattering, (b) Forward scattering.

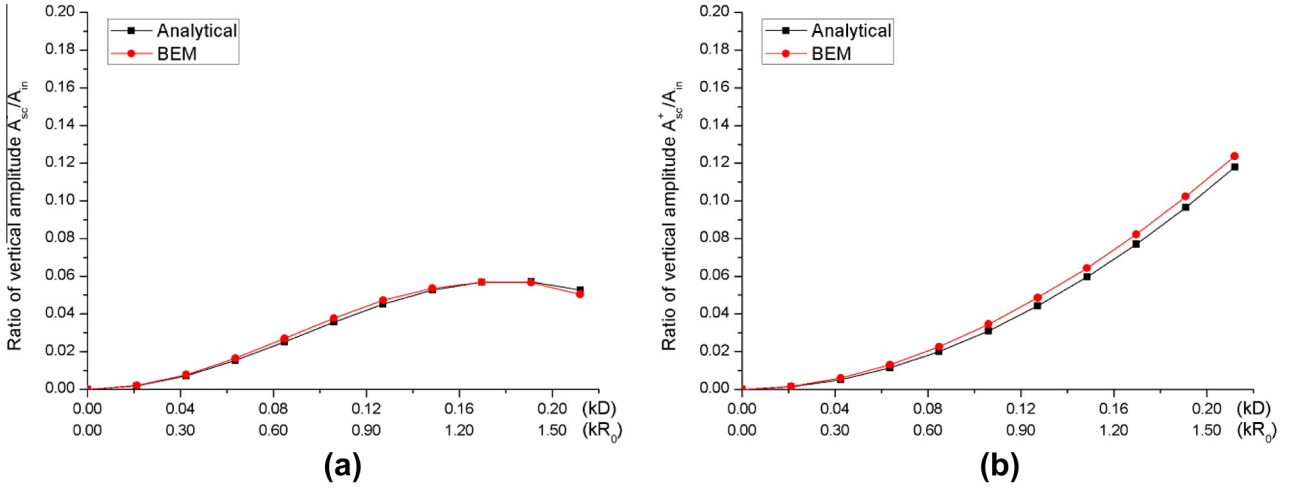

Fig. 6. Scattering by a cylindrical cavity; $R_0 = 0.75$ mm, $D = 0.10$ mm, 0.1 MHz $\leq f \leq$ 1.0 MHz; (a) Backscattering, (b) Forward scattering.

$R_0 \geq D$. The material is steel, which has a shear modulus of $\mu = 7.9872 \times 10^{10}$ N/m^2, a Lame's constant of $\lambda = 11.03 \times 10^{10}$ N/m^2, and a density of $\rho = 7800$ kg/m^3. In the following representation of the results, we have fixed the depth D and the width R_0 for each case of calculation, and we have varied the frequency from $f = 0.1$ MHz to $f = 1.0$ MHz so that kD and kR_0 also vary. The values of $|A_{sc}^-/A_{in}|$ and $|A_{sc}^-/A_{in}|$ are then only dependent on the dimensionless quantities kD and kR_0.

We first consider four cases of study in which the cavities have the same $D = 0.10$ mm, and different R_0, where $R_0 = 0.50$ mm in Fig. 5a and b, $R_0 = 0.75$ mm in Fig. 6a and b, $R_0 = 1.00$ mm in Fig. 7a and b, and $R_0 = 1.25$ mm in Fig. 8a and b so that R_0/D has values of 5.0, 7.5, 10.0 and 12.5, respectively. The frequency varies from $f = 0.1$ MHz to $f = 1.0$ MHz.

The comparisons between the analytical and the BEM results for the absolute values of the amplitude ratios of the scattered field to the incident field are in good agreement in Figs. 5 and 6a and b. When R_0 increase from $R_0 = 0.50$ mm and $R_0 = 0.75$ mm in Figs. 5 and 6a and b to $R_0 = 1.00$ mm and $R_0 = 1.25$ mm in Figs. 7 and 8a and b, the comparisons become even better with excellent agreement, especially for the forward scattering. Fig. 8a shows a slight difference between the analytical and the BEM results for the backscattering when $kR_0 \geq 2.0$. This is due to for the existence of the term $e^{-2i\bar{x}_0}$, where $\bar{x}_0 = kx_0$ in Eq. (57).

We now consider two cavities with the same $R_0 = 1.00$ mm and different D where $D = 0.20$ mm in Fig. 9a and b and $D = 0.30$ mm in Fig. 10a and b, respectively, and compare with the results for $R_0 = 1.00$ mm, $D = 0.10$ mm plotted in Fig. 7a and b. The frequency varies from $f = 0.1$ MHz to $f = 1.0$ MHz.

When D increases from $D = 0.10$ mm in Fig. 7a and b to $D = 0.20$ mm in Fig. 9a and b, and $D = 0.30$ mm in Fig. 10a and b, the analytical approximation begins to diverge from the solution obtained by the BEM for both the backscattering and the forward scattering. This shows the limitation of the analytical approximation with increase of the depth of the cavity.

We now consider two other cases in which the cavities have the same $R_0/D = 10.0$ as in Fig. 7a and b, but now with larger values of both D and R_0. In Fig 11a and b, $D = 0.15$ mm, $R_0 = 1.50$ mm and in Fig. 12a and b, $D = 0.2$ mm, $R_0 = 2.00$ mm. The frequency varies from $f = 0.1$ MHz to $f = 1.0$ MHz.

In Fig. 7b, the analytical solutions and the BEM results show same excellent agreement for the forward scattering as the comparisons. For $kR_0 \leq 2.0$, we also have the same excellent agreement for backscattering shown in Figs. 11 and 12a, as in Fig. 7a. For

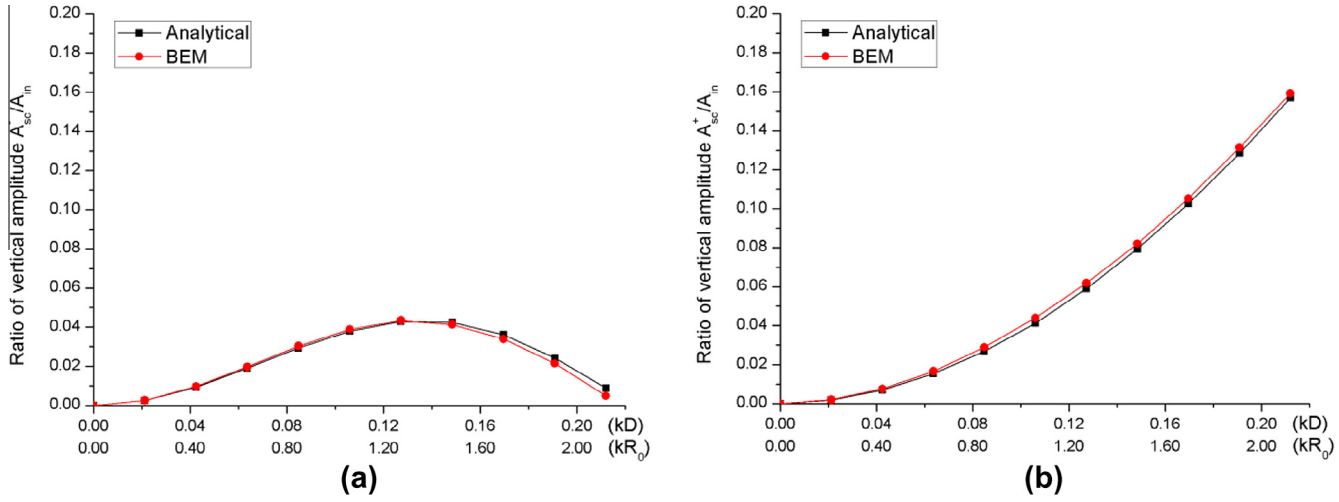

Fig. 7. Scattering by a cylindrical cavity; $R_0 = 1.00$ mm, $D = 0.10$ mm, 0.1 MHz $\leq f \leq$ 1.0 MHz; (a) Backscattering, (b) Forward scattering.

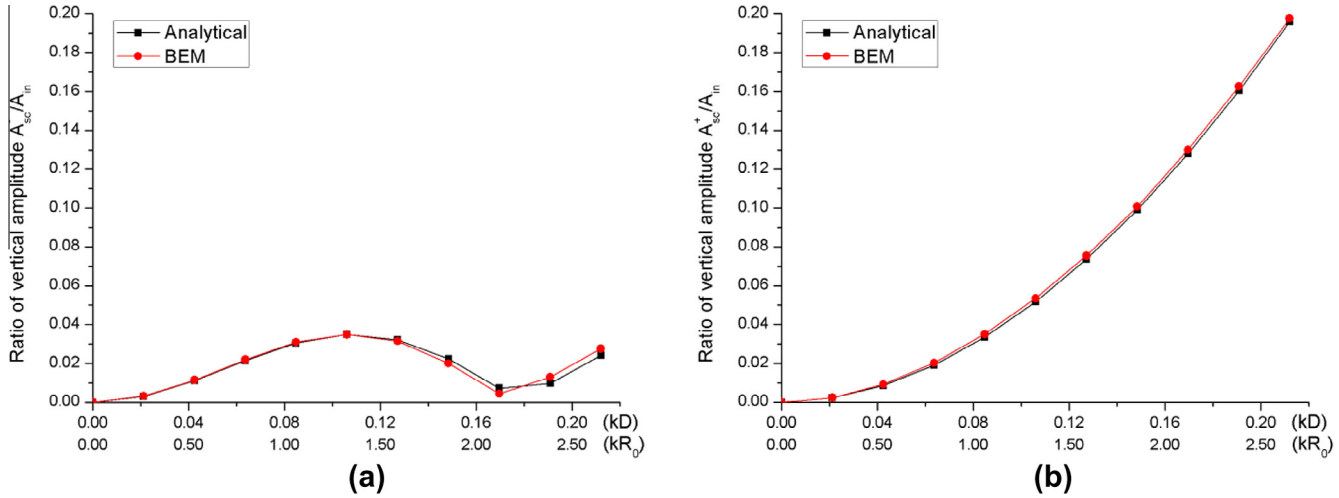

Fig. 8. Scattering by a cylindrical cavity; $R_0 = 1.25$ mm, $D = 0.10$ mm, 0.1 MHz $\leq f \leq$ 1.0 MHz; (a) Backscattering, (b) Forward scattering.

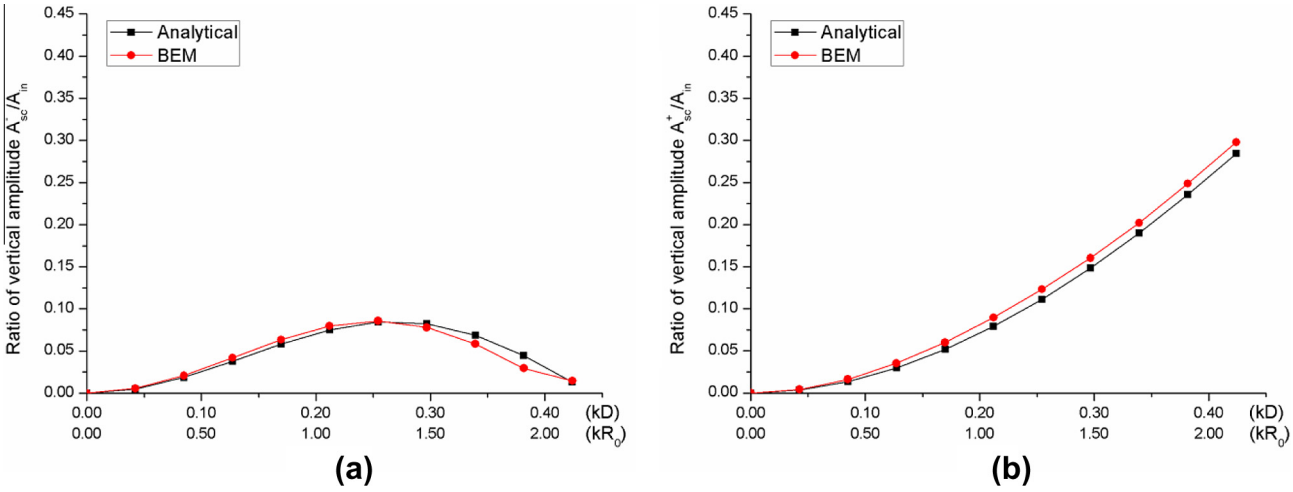

Fig. 9. Scattering by a cylindrical cavity; $R_0 = 1.00$ mm, $D = 0.20$ mm, 0.1 MHz $\leq f \leq 1.0$ MHz; (a) Backscattering, (b) Forward scattering.

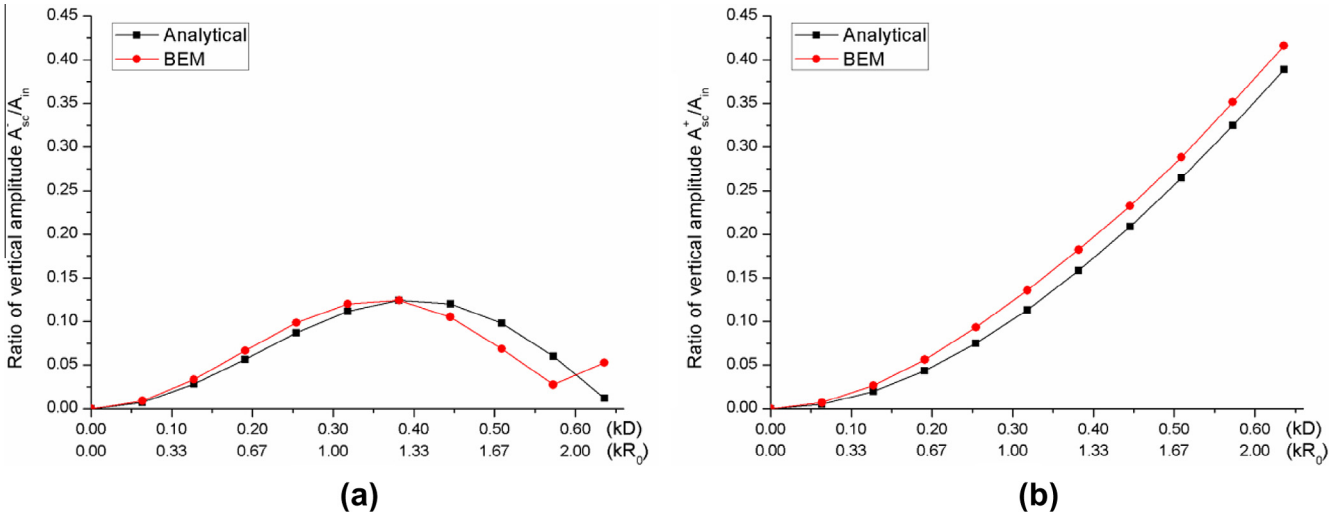

Fig. 10. Scattering by a cylindrical cavity; $R_0 = 1.00$ mm, $D = 0.30$ mm, 0.1 MHz $\leq f \leq 1.0$ MHz; (a) Backscattering, (b) Forward scattering.

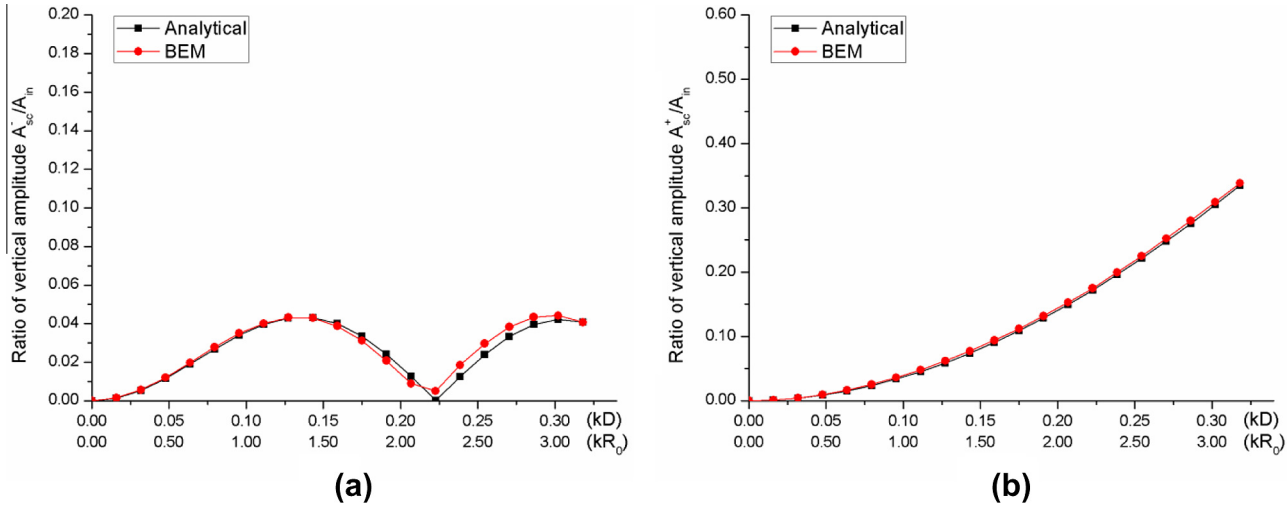

Fig. 11. Scattering by a cylindrical cavity; $R_0 = 1.50$ mm, $D = 0.15$ mm, 0.1 MHz $\leq f \leq 1.0$ MHz; (a) Backscattering, (b) Forward scattering.

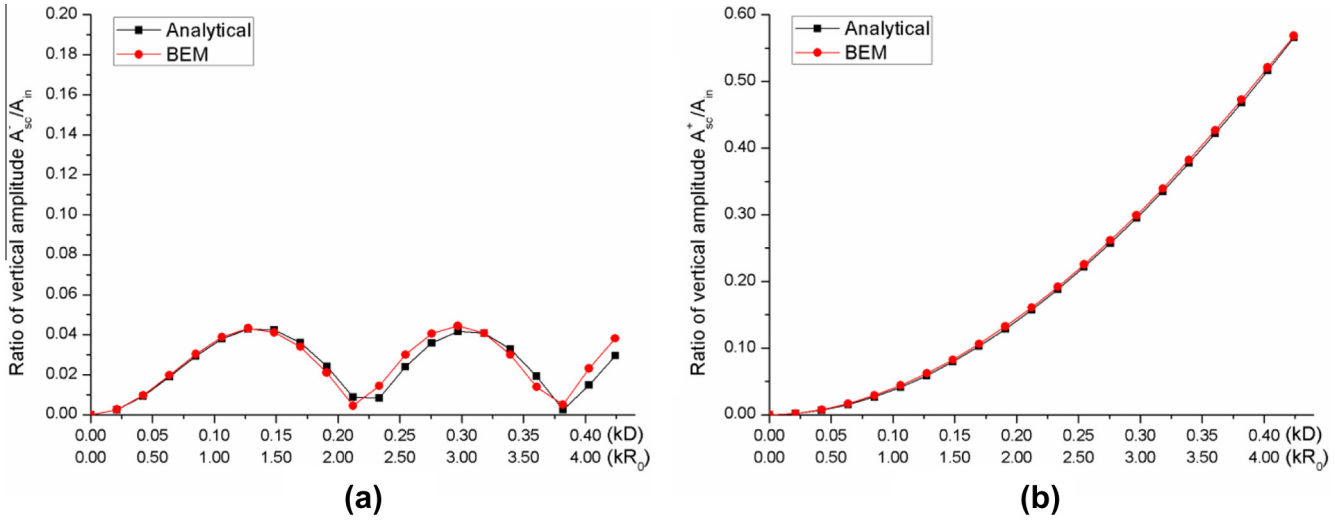

Fig. 12. Scattering by a cylindrical cavity;$R_0 = 2.00$ mm, $D = 0.20$ mm, 0.1 MHz $\leq f \leq$ 1.0 MHz; (a) Backscattering, (b) Forward scattering.

$kR_0 \geq 2.0$, the analytical solutions become slightly different from the BEM results. This, as mentioned before, is due to the existence of the term $e^{-2i\bar{x}_0}$ where $\bar{x}_0 = kx_0$ in Eq. (57).

The comparisons between the analytical and BEM results from Figs. 5–12a and b show not only excellent agreement but also slight differences for different cavities. It shows that the analytical approach presented in this paper has limitations. In summary, for the forward scattering, agreement between the analytical solutions and the BEM results only depends on the ratio kR_0/kD. The bigger kR_0/kD, the better agreement of the comparisons. Excellent agreement has been shown in Figs. 7, 11 and 12b for $kR_0/kD = 10.0$. With smaller kR_0/kD, for example $kR_0/kD = 3.3$, comparisons between the analytical and the BEM results are in good agreement but have about 8–10% difference as shown in Fig. 10b. Meanwhile, for the backscattering, agreement between the analytical solutions and the BEM results depends on both the ratio kR_0/kD and kR_0 itself. For $kR_0/kD = 10$, comparisons for the backscattering are in excellent agreement for $kR_0 \leq 2$ as shown in Figs. 7, 11 and 12a. They are just slight different when $kR_0 > 2$. With $kR_0/kD = 3.3$, as in Fig. 10a, comparisons are in good agreement and have about 8–10% difference when $kR_0 \leq 1.5$. For $kR_0 \geq 1.5$, they are not in very good agreement.

In conclusion it has been shown in this paper that by using the elastodynamic reciprocity theorem, the scattering of surface waves by a two-dimensional cavity in an elastic half-space can be solved in a simple manner. We have theoretically derived the ratios of the vertical displacement amplitudes of the scattered surface waves to those of the incident surface waves in terms of dimensionless quantities. The ratios do not depend (independently from kR_0 and kD) on f. The comparisons with BEM results provide validation of the analytical approximation for certain ranges of the parameters kD and kR_0. The proposed theoretical approach has given very good results for the cylindrical cavity through the examples presented in this paper. However, under certain conditions of kR_0 and kD, different cavity geometries may also be expected to give good results.

Acknowledgement

This work was supported by Radiation Technology R&D program through the National Research Foundation of Korea funded by the Ministry of Science, ICT & Future Planning (2013M2A2A9043241).

References

Abrahams, I.D., Wickham, G.R., 1992. Scattering of elastic waves by an arbitrary small imperfection in the surface of a half-space. J. Mech. Phys. Solids 40, 1683–1706.
Achenbach, J.D., 1973. Wave Propagation in Elastic Solids. North-Holland Publishing Company.
Achenbach, J.D., 2000. Calculation of wave fields using elastodynamic reciprocity. Int. J. Solids Struct. 37, 7043–7053.
Achenbach, J.D., 2003. Reciprocity in Elastodynamics. Cambridge University Press.
Arias, I., Achenbach, J.D., 2004. Rayleigh wave correction for the BEM analysis of two-dimensional elastodynamic problems in a half-space. Int. J. Numer. Methods Eng. 60, 2131–2146.
Auld, B.A., 1979. General electromechanical reciprocity relations applied to the calculation of elastic wave scattering coefficients. Wave Motion 1, 3–10.
Cho, Y., Rose, J.L., 2000. An elastodynamic hybrid boundary element study for elastic guided wave interactions with a surface breaking defect. Int. J. Solids Struct. 37, 4103–4124.
Ewing, W.M., Zardetzky, W.S., Press, F., 1957. Elastic Waves in Layered Media. McGraw-Hill.
Gilbert, F., Knopoff, L., 1960. Seismic scattering from topographic irregularities. J. Geophys. Res. 65, 3437–3444.
Gregory, R.D., Austin, D.M., 1990. Scattering of waves by a semicylindrical groove in the surface of an elastic half-space. Q. J. Mech. Appl. Math. 43, 293–315.
Hao, S., Strom, B.W., Gordon, G., Krishnaswamy, S., Achenbach, J.D., 2011. Scattering of the lowest lamb wave modes by a corrosion pit. Res. Nondestruct. Eval. 22, 208–230.
Hassan, W., Veronesi, W., 2003. Finite element analysis of Rayleigh wave interaction with finite-size, surface-breaking cracks. Ultrasonics 41, 41–52.
Kosachev, V.V., Lokhov, Y.N., Chukov, V.N., 1990. On the theory of scattering the Rayleigh surface acoustic waves by a two-dimensional statistical roughness of a free solid surface. Solid State Commun. 73, 535–539.
Lamb, H., 1904. On the propagation of tremors over the surface of an elastic solid. Philos. T. Roy. Soc. A 203, 1–42.
Moreau, L., Castaings, M., 2008. Scattering of lamb waves by a complex shaped defect in an isotropic plate. AIP Conf. Proc. 975, 62–69.
Ogilvy, J.A., 1987. Wave scattering from rough surfaces. Rep. Prog. Phys. 50, 1553.
Phan, H., Cho, Y., Achenbach, J.D., 2013. Validity of the reciprocity approach for determination of surface wave motion. Ultrasonics 53, 665–671.
Rayleigh, L., 1885. On waves propagated along the plane surface of an elastic solid. Proc. Lond. Math. Soc. s1–17, 4–11.
Simons, D.A., 1978. Reflection of Rayleigh waves by strips, grooves, and periodic arrays of strips or grooves. J. Acoust. Soc. Am. 63, 1292–1301.
Tuan, H.-S., Li, R.C.M., 1974. Rayleigh-wave reflection from groove and step discontinuities. J. Acoust. Soc. Am. 55, 1212–1217.
Viktorov, I.A., 1970. Rayleigh and Lamb Waves: Physical Theory and Applications. Plenum Press.